Available online at www.sciencedirect.com

ScienceDirect

Materials Today: Proceedings 15 (2019) 464–470

materialstoday: PROCEEDINGS

www.materialstoday.com/proceedings

ICMAM-2018

Samarium doped ZnO nanofibers for designing orange - red light emitting fabrics

Chaitali N. Pangul[a], Shyamkant W. Anwane[b], Subhash B. Kondawar[a]*

[a]Department of Physics, Rashtrasant Tukadoji Maharaj Nagpur University, Nagpur, India
[b]Department of Physics, Shri Shivaji Science College, Nagpur, India

Abstract

In this paper, we report the orange - red luminescence from samarium doped ZnO nanofibers fabricated by Electrospinning. The as-prepared samarium doped ZnO nanofibers was examined by XRD, SEM-EDX, UV-VIS and FTIR characterizations. XRD revealed the presence of sharp peaks of ZnO in agreement with hexagonal wurtzite ZnO peaks. SEM explored the formation of ultralong smooth nanofibers. EDX revealed the presence of Zn, O and Sm peaks confirms the formation of samarium doped ZnO nanofibers. The band gap energy of samarium doped ZnO nanofibers was found to be increasing from 3.7 eV to 3.8 eV with increase in concentration of dopant as computed by UV-Vis spectroscopy. An eminent stretching bond of Zn-O was observed in prepared nanofibers by FTIR spectroscopy. A very bright orange-red luminescence was observed upon excitation at 394nm in photoluminescence study of samarium doped ZnO nanofibers. The resulting luminescence is result of two prominent peaks due to magnetically allowed transition $^4G_{5/2} \rightarrow {}^6H_{7/2}$ and electrically forced transition $^4G_{5/2} \rightarrow {}^6H_{9/2}$. These are the distinctive peaks of dopant Sm^{3+} ions. It is interesting to see the luminescence is from dopant while the host's defect luminescence is latent. This disguised the operative energy transfer from host ZnO to dopant Sm^{3+} ion. From the colour parameters calculated by CIE analysis, the prepared samarium doped ZnO nanofibers is suitable for designing the orange-red light emitting fabrics

Selection and Peer-review under responsibility of INTERNATIONAL CONFERENCE ON MULTIFUNCTIONAL ADVANCED MATERIALS (**ICMAM-2018**).

Keywords: Nanofibers; Electrospinning; Photoluminescence; Samarium; Zinc Oxide.

*Email address: sbkondawar@yahoo.co.in

Selection and Peer-review under responsibility of INTERNATIONAL CONFERENCE ON MULTIFUNCTIONAL ADVANCED MATERIALS (**ICMAM-2018**).

1.0 Introduction

The term nanomaterials itself comprises a wide aspect of opportunities for the development and benefits of society. Nanomaterials embrace quantum dots, 1-D nanowires, nanorods, nanofibers, and nanotubes, and 2-D nanosheets. Extensively observed as nanomaterials with extraordinary applications, nanofibers show up among the rest of the nanomaterials. High surface area-to-volume ratio and high porosity are the most prominent features of nanofibers making them a full-bodied and striking candidate for many advanced applications [1]. Various methods including sol–gel, co-precipitation, hydro- thermal route and spray pyrolysis have been widely employed in the fabrication of nanoscale geometries such as thin films, nanoparticles, nanorods and nanofibers [2]. Besides these all Electrospinning has been most accredited method for fabrication of nanofibers. Nanofibers demonstrate splendid properties owing variety of applications such as sensors, energy cells, super capacitors, light emitting displays, etc. [3, 4]. Despite, tremendous work on Light emitting devices is carried out, light emission from flexible nanomaterials has been under recurrent process of research. Light emitting fibers had noticeable place in Light emission research fields [5]. ZnO had been always a part of all-embracing research owing to its wide band gap (3.34eV) and high binding energy (60meV) [6, 7]. ZnO is virtuous candidate of applications in piezoelectric transducers, transparent field-effect transistors, gas sensors, optical waveguides, transparent conductive films, ultraviolet Nano lasers, varistors, photodetectors, solar cells, blue and ultraviolet (UV) optical devices, and bulk acoustic wave devices [8]. Furthermore, ZnO has also been host of choice for diversity of dopants. Doping of various materials in ZnO had emerged ZnO as a very probable aspirant for variety of applications [9]. Doping of Rare earth elements has enhanced the optical properties of Zinc Oxide in abundant way [10, 11]. Jingyuan Piao et. al had studied ferromagnetism in Sm doped ZnO nanorods [12]. Manjeet Kumar et. al had achieved maximum photo response in terms of sensitivity for an optimum Sn doping level in ZnO [13]. Hung-Pin Hsu et. al had found enhanced photo-to-dark-current ratio with increasing Li doping in ZnO films [14]. Krisana Kobwittaya et.al observed bright red up conversion luminescence from Er^{3+} and Yb^{3+} co-doped ZnO-TiO2 composite phosphor powder [15]. Jingjing Jiang et. al observed enhanced photodegradation activity for artificial waste water for Porous Ce-doped ZnO hollow sphere structures [16]. In our previous work we observed enhanced white luminescence from Dy^{3+} doped ZnO nanofibers.

In this work we primarily focused on the colour luminescence owed to defect free emission from variety of doping in ZnO. We synthesized Samarium doped ZnO nanofibers utilizing electrospinning technique and observed orange-red colour emission. Enhanced orange-red defect free emission from ZnO nanofibers was observed.

2.0 Experimental

0.5 g $Zn(CH_3COO)_2.H_2O$ and x% ($Sm(NO_3)_3$) (x=1,2) were dissolved in deionised water. 0.35 g of PVA and 0.059 g acetic acid were added and stirred magnetically at 60ºC for 2 h. The solution was filled in the disposable 5 ml syringe for electrospinning. The distance between the syringe needle tip and collector aluminium foil was fixed at 15 cm. The flow rate of the solution was 0.4 ml/h and controlled by microprocessor based syringe pump. The electric field between the syringe needle tip and collector aluminium foil was maintained at 18 kV. The fibers were collected on the aluminium foil and pilled off for drying. The fibers were then calcined at 300 °C for 2 h in muffle furnace. The as-prepared fibers were characterized by scanning electron microscopy (SEM) equipped with energy dispersive x-ray spectroscopy (Carl Ziess EVO 18), x-ray diffraction (XRD) with Cu Kα target (λ = 1.5418Aº) Rigaku, Miniflex 600, ultraviolet visible spectroscopy (UV-VIS, Carry 5000), Fourier transform infra red spectroscopy (ThermoNicolet, Avatar 370) and photoluminescence (Shimadzu RF-5301PC).

3.0 Results and Discussion

Fig. 1 shows the X-Ray Diffraction patterns of x% Samarium doped ZnO nanofibers (x =1, 2) calcined at 300 ºC. Hexagonal wurtzite structure of Zinc Oxide (JCPDS No. 36-1451) is confirmed by the distinctive diffraction peaks observed in the sample. Peaks related to Sm_2O_3 or $Zn(OH)_2$ are not detected which approves that Sm^{3+} have been effectively merged into ZnO.

Fig. 2 (a) and Fig. 2(b) represents the SEM images of calcined x% Samarium doped ZnO nanofibers (x =1, 2) calcined at 300 °C. Observing SEM images disclose that ultra long, continuous, even and uniform with random alignments nanofibers. Upon calculating the average diameter from frequency distribution diagram of 1% Samarium

doped ZnO nanofibers and 2% Samarium doped ZnO nanofibers, it was found to be 350 nm and 270 nm respectively. Even when the PVA was parted away by calcinations, the prepared samples remain as the continuous inorganic fibres. Fig 3 is the EDX spectra of the Samarium doped ZnO nanofibers calcined at 300ºC which confirm the occurrence of elemental Zn, O and Sm in electrospun nanofibers.

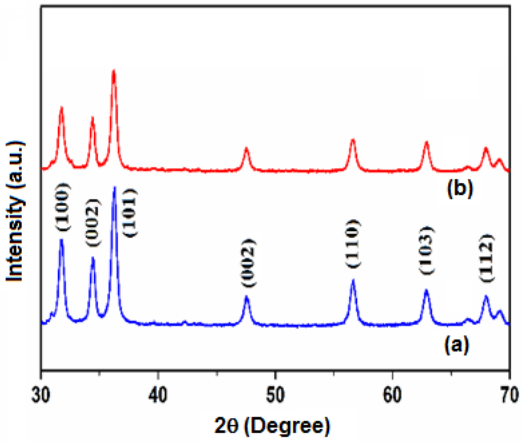

Fig. 1: XRD patterns of samarium (a) 1% and (b) 2% doped ZnO nanofibers

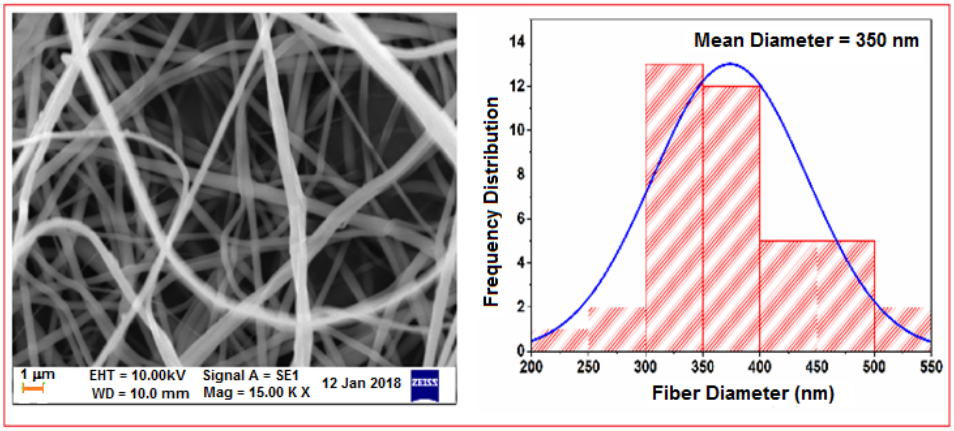

Fig. 2(a): SEM image of 1% Samarium doped ZnO nanofibers

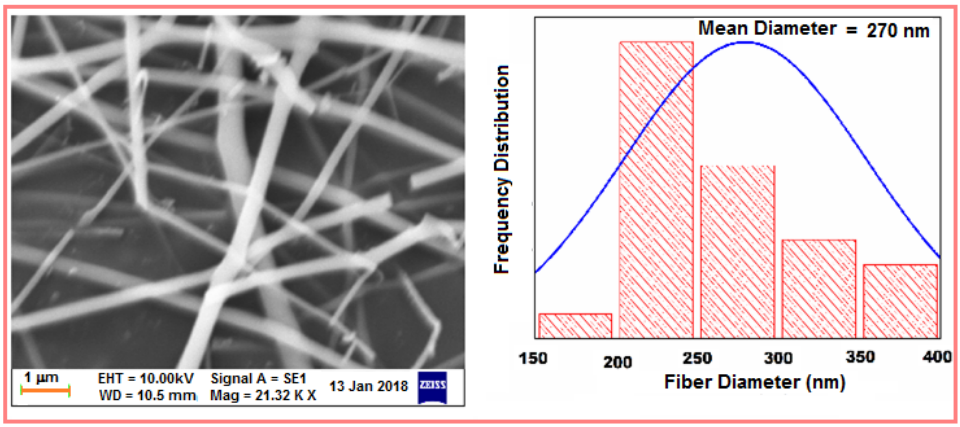

Fig. 2(b): SEM image of 2% Samarium doped ZnO nanofibers

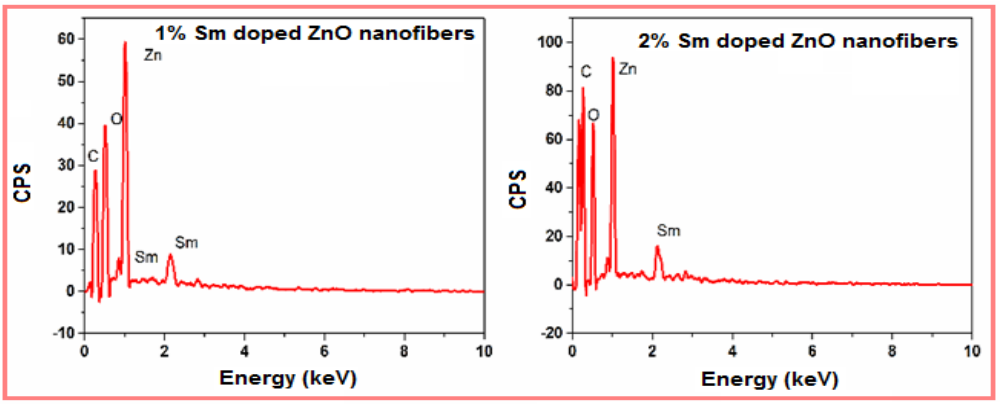

Fig. 3: EDX spetra of calcined x% Samarium doped ZnO nanofibers (x = 1, 2)

UV- Vis spectroscopic studies had been carried out to study the effect of doping on the band gap properties of ZnO [17]. Fig.4 (a) and Fig.4 (b) shows the UV-Vis absorption spectra along with Tauc's plot of 1% and 2% Samarium doped ZnO nanofibers calcined at 300°C respectively. A very strong absorption is observed at 390nm in both the samples of Samarium doped ZnO nanofibers. This resembles the absorption properties of ZnO at an UV wavelength. Optical band gap is calculated using Tauc' s plot [18]. Following equation gives the frequency dependent absorption coefficient ,

$$(\alpha h\nu)^{\frac{1}{n}} = A(h\nu - E) \qquad (1)$$

Where, Beer- Lambert's relation $\alpha = 2.303A/d$ is used to calculate α which is the absorption coefficient while A is the Absorbance and d is the thickness of the film respectively. $h\nu$ and E are the incident photon energy and optical band gap. For a direct band gap semiconductor like ZnO the graph between $(\alpha h\nu)^2$ and hν gives the Tauc's plot and extrapolating $(\alpha h\nu)^2 = 0$ gives the value of optical band gap of direct band gap semiconductor[19]. From Tauc's plot it is very evident that the optical band gap was found to increase with the doping concentration from 3.707eV to 3.81eV. It would be interesting to note here that the band gap energy even goes on increasing with reducing diameters of nanofibers. Band gap of the material can be tuned with the variation of diameter of nanofibers.

Fig.5 represents the FTIR spectra of (a) 1% and (b) 2% Samarium doped ZnO nanofibers calcined at 300°C. Surely an intense absorption band at 443 cm^{-1} in 1% Sm doped and at 449 cm^{-1} in 2% Sm doped are associated with stretching vibration of metal bond (Zn-O). Another peak at 493 cm^{-1} could be ascribed to the oxygen deficiency and /or defect states in ZnO [20, 21].

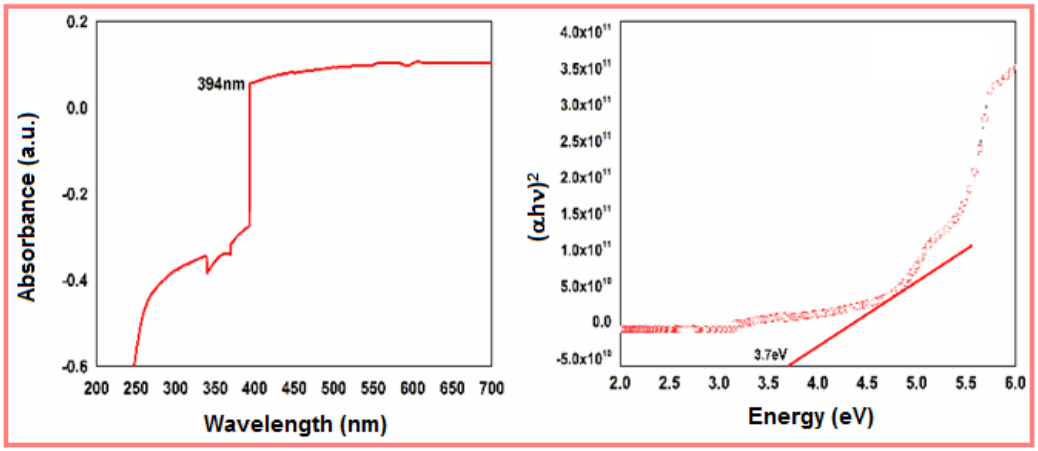

Fig. 4(a): UV-Vis absorption spectra and Tauc's plot of $(\alpha h\nu)^2$ vs hν of 1% Sm^{3+} doped ZnO nanofiber

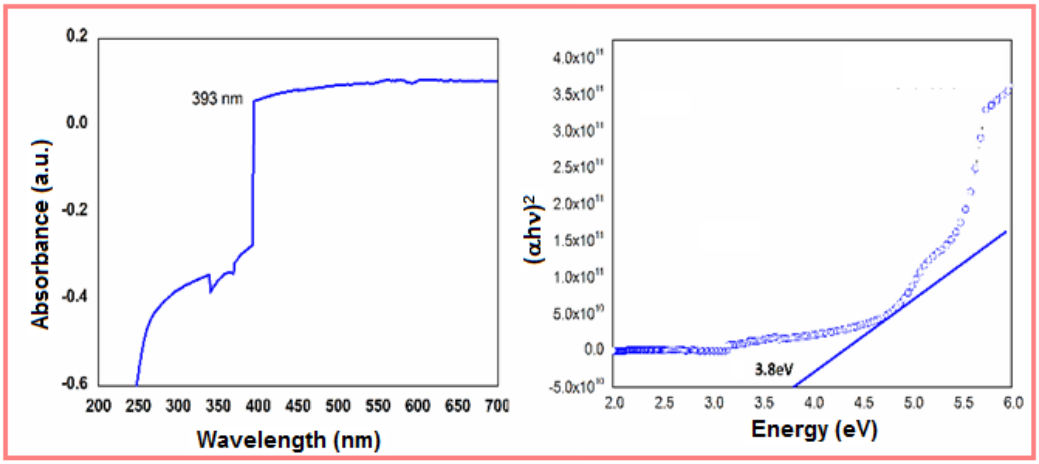

Fig. 4(b): UV-Vis absorption spectra and Tauc's plot of $(\alpha h\nu)^2$ vs hν of 2% Sm^{3+} doped ZnO nanofiber

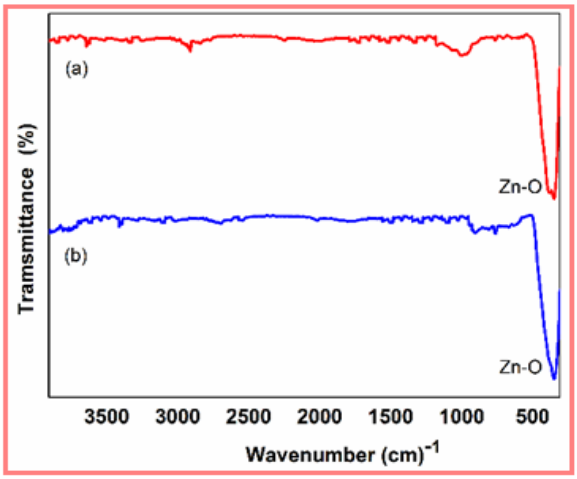

Fig. 5: FTIR spectra (a) 1% and (b) 2% Samarium doped and (2%) ZnO nanofibers

Fig. 6 shows the PL spectra of Samarium doped ZnO nanofibers respectively for (a) 1% and (b) 2% doping. It is clearly observed, when excited at an excitation wavelength 394 nm two spectral peak around 606nm and 644 nm are observed in both Samarium ion doped ZnO nanofibers which represents the distinctive emission peak of Sm^{3+} ions. With respect to Samarium, peak at 606nm represent magnetically allowed $^4G_{5/2} \rightarrow {}^6H_{7/2}$ transition while another peak at 644nm is electrically forced $^4G_{5/2} \rightarrow {}^6H_{9/2}$ transition [22]. Excitation spectra was recoded at 606nm which gives a broad peak around 390nm, the absorption maxima. In our previous work ZnO nanofibers exhibit visible emission owing to characteristic UV and defect green emission [23]. It is noteworthy here to explain that no emission from defect states of ZnO is observed [24]. This could be explained as a part of operative and effectual energy transfer mechanism from host ZnO to dopant Sm^{3+} ion [25]. Upon excitation at an absorption wavelength of ZnO, the host gets excited and in arrival transfer its energy to the dopant ion which while coming back to ground state emits obeying its characteristic transitions. It is also important to notice that the intensity is increasing with the dopant concentration.

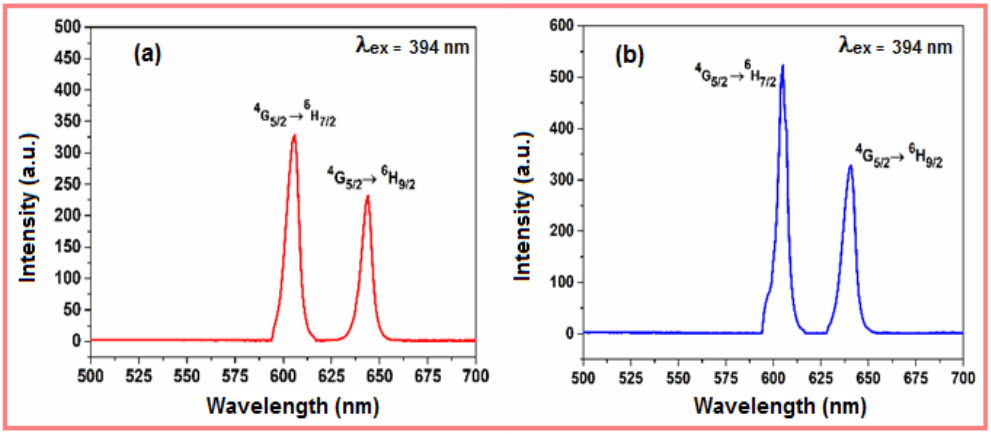

Fig. 6: Photoluminiscence emission spectra of (a) 1% and (b) 2% Samarium doped ZnO nanofibers

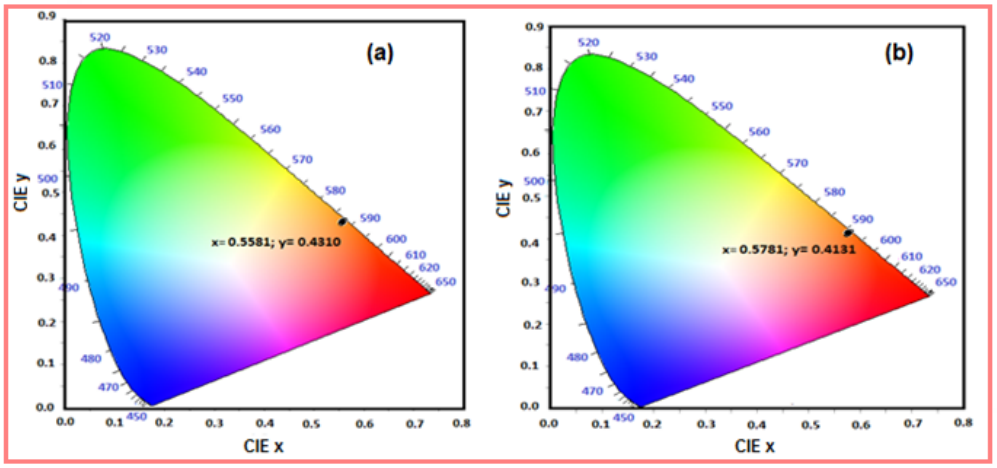

Fig. 7 (a): CIE diagram of (a) 1% and (b) 2% Samarium doped ZnO nanofibers

The Photometric characteristics of the prepared nanofibers were studied along with CIE parameters such as colour coordinates, colour co-related temperature (CCT), Colour Rendering Index (CRI) and Luminescence Efficacy of Radiation (LER). Fig. 7(a) and Fig. 7(b) illustrates the CIE chromaticity diagram of emission spectra of Samarium doped ZnO nanofibers. Spectral Energy distribution of Chromaticity diagram was used to calculate the parameters by spectrophotometric method was used to calculate the parameters and are summarized in Table 1. The colour coordinates (x;y) were calculated using the standard procedure [26]. Performance of luminescent materials can be verified by their Colour Co- ordinates. From chromaticity diagram, it is seen that the co-ordinates lie in the orange-red. It is apparent from obtained values of CCT, CRI and LER as in Table.1, Samarium doped ZnO nanofibers are apt candidates for use in orange- red light emitting devices.

Table 1: Photometric characteristics of prepared nanofibers.

Sm^{3+} doped ZnO nanofibers	CIE y	CCT	LER (lm/W)	CRI (Ra)
1% Sm^{3+} doped	0.4310	1866	342	68
2% Sm^{3+} doped	0.4131	1642	330	66

4.0 Conclusions

Samarium doped ZnO nanofibers with diameters ranging upto 250 to 350 nm have been fabricated successfully utilising the technique of Electrospinning. An functioning energy transfer from ZnO to Sm^{3+} ion is observed from the Photoluminescence studies. Enhanced visible light luminescence in orange-red region is observed in CIE diagram. Hence colour tunability is found to be factor depending upon type of dopant for ZnO. This kind of materials are expected to be used in visible light emitting devices rather its form of fibres enables its uses in variety of applications such as flexible light emitting displays, banners, smart clothing, etc. Furthermore, it would be interesting to study the effect of various dopants in ZnO nanofibers and effect of various calcination temperatures on the luminescence intensity.

References

1. Kenry, C. T. Lim, Prog. Polym. Sci. 70(2017)1–17.
2. M. AbiJaoude, K. Polychronopoulou, S. J. Hinder, M. S. Katsiotis, M. A. Baker, S. M. Alhassan, Ceram. Int. 42(2016)10734–10744.
3. L. Udom, M. K. Rama, E. K. Stefanakos, A. Hepp, F. D. Y. Goswami, Mater. Sci. Semi. Proc. 16(2013)2070–2083.
4. M. F. Lin, J. Xiong, J. Wang, K. Parida, P. S. Lee, Nano Ener. 44(2018)248–255.
5. M. P. Dandekar, S. B. Kondawar, S. G. Itankar, D. V. Nandanwar, Proc. Mater. Sci. 10(2015)580 –587.
6. Y. S. Park, C. W. Litton, T. C. Collins, D. C. Reynolds, Phy. Rev. 143(1966)512.
7. W. C. Uang, J. L. Chiu, X. D. Lin, Y. C. Lin, S. C. Tsai, W. M. Su, C. Y. Weng, C. F. Lu, H. Chen, Result. Phys. 10(2018)132-137.
8. K. Badreddine, I. Kazah, M. Rekaby, R. Awad, J. Nanomater. 7096195(2018)1-11.
9. A. Ievtushenko, V. Karpyna, J. Eriksson, I. Tsiaoussis, L. Shtepliuk, G. Lashkarev, R. Yakimova, Khranovskyy, Superlattice. Microstruct. 117(2018)121-131.
10. A. Balakrishnaa, T. K. Pathak, E. C. Hugo, R. E. Kroon, O. M. Ntwaeaborwa, H. C. Swart, Colloids Surf. A Physicochem. Eng. Asp. 540(2018)123-135.
11. M. Babamoradi, H. Sadeghi, R. Azimirad, S. Safa, Optik. 67(2018)88–94.
12. J. Piao, L. T. Tseng, J. Yi, Chem. Phys. Lett. 649(2016)19-22.
13. M. Kumar, V. Bhatt, A. C. Abhyankar, J. Kima, A. Kumar, J. H. Yun, Sens. Actuat. A 270(2018)118-126.
14. H. P. Hsu, D. Y. Lin, C. Y. Lu, T. S. Ko, H. Z. Chen, Crystals. 8(2018)228-234.
15. K. Kobwittaya, Y. Oishi, T. Torikai, M. Yad, T. H. Watari, N. Luitel, Ceram. Int. 43(2017)13505-13515.
16. J. Jiang, K. Zhang, X. F. Chen, T. Xie, D. Wang, Y. Lin, J. Alloy. Comp. 699(2017)907-913.
17. R. N. Ali, H. Naz, J. Li, X. Zhu, P. Liu, B. Xiang, J. Alloy. Comp. 744(2018)90-95.
18. V. Anand, A. K. Sakthivelu, D. A. Kumar, S. Valanarasu, A. Kathalingam, V. Ganesh, M. Shkir, S. A. Faify, I. S. Yahia, Ceram.Int. 44(2018)6730–6738.
19. S. M. Park, T. Ikegami, K. Ebihara, Thin Solid Film. 513(2006)90–94.
20. T. K. Mandal, S. P. K. Malhotra, R. K. Singha, R. K. Roman. J. Mater. 48(2018) 32 -38 .
21. G. Xiong, K. B. Ucer, R. T. Williams, U. Pal, J. G. Serrano, Phys. Stat. Sol. 2(2003)711-714.
22. M. Seshadri, M. Radha, D. Rajesh, L. C. Barbosa, C. M. B. Cordeiro, Y. C. Ratnakarama, Physica B. 459(2015)79–87.
23. C. N. Pangul, S. W. Anwane, S. B. Kondawar, Lumin. 33(2018)1087-1093.
24. D. Ranjith Kumar, K. S. Ranjith, R. T. R. Kumar, Optik. 154(2018)115–125.
25. E. Sreeja, S. Gopi, V. Vidyadharan, P. R. Mohan, C. Joseph, N. V. Unnikrishnan, P. R. Biju, Powder Technol. 323(2018)445–453.
26. R. Furue, K. Matsuo, Y. Ashikari, H. Ooka, N. Amanokura, T. Yasuda, Adv. Optical Mater. 6(2018)1701147.